Electronic transitions associated with small crystalline silicon inclusions within an amorphous silicon host

Daewon Kwon, Chih-Chiang Chen, and J. David Cohen
Department of Physics, University of Oregon, Eugene, Oregon 97403

Hyun-Chul Jin, Eric Hollar, Ian Robertson, and John R. Abelson
Coordinated Science Laboratory and Department of Materials Science and Engineering, University of Illinois, Urbana, Illinois 61801

(Received 4 December 1998; revised manuscript received 3 May 1999)

Amorphous silicon films were prepared by dc reactive magnetron sputtering under a range of hydrogen or deuterium partial pressures approaching the phase transition to full microcrystallinity. Tunneling electron microscopy imaging indicated that these films consisted of 5–50-nm-sized Si crystallites embedded in an amorphous silicon matrix. The sub-band-gap optical spectra of these films were recorded using photocapacitance and transient photocurrent spectroscopy. These spectra appear to consist of a superposition of a sub-band-gap spectrum typical of amorphous silicon together with a unique optical transition, with a very large optical cross section, corresponding to valence-band electrons being optically inserted into empty levels lying within the amorphous silicon mobility gap. We believe these empty levels are associated with defect states at the crystalline-amorphous boundary. [S0163-1829(99)08331-9]

Shortly after the development of hydrogenated amorphous silicon (a-Si:H) with good electronic properties using the glow discharge and sputtering growth methods, these same methods were shown to be able to produce microcrystalline Si (μc-Si) at the same low temperatures as the amorphous films.[1–5] Films just below the amorphous/crystalline phase boundary have recently been attracting considerable interest since these appear to be the most stable with respect to light-induced degradation in photovoltaic devices.[6,7] It is also known that once the μc-Si volume fraction becomes appreciable, the performance of such devices suffers considerably.[6,8]

In this paper we report results from a study of samples produced by dc sputtering under hydrogen or deuterium dilution. Tunneling electron microscopy (TEM) confirmed that these samples contain Si microcrystallites embedded in an amorphous silicon host matrix. The electronic properties of these samples were characterized by photocapacitance and photocurrent methods to reveal a unique optical transition associated with the embedded crystallites. This transition, which behaves like a defect level within the amorphous silicon host with an unusually large optical cross section, is very likely to impact the performance of devices employing such mixed phase materials.

Both hydrogenated and deuterated films were deposited at a rate of 100 Å/min by dc reactive magnetron sputtering of a 5×12 in.^{2} planar Si target in an $Ar+H_2$ or $Ar+D_2$ plasma. The substrate temperature was 250 °C, the Ar partial pressure was 0.14 Pa, and the H_2 or D_2 pressure was varied from 0.04 to 0.10 Pa. Films grown under such conditions using hydrogen have been found to have properties fully equivalent to a-Si:H deposited by plasma CVD.[9] Previous studies have determined that the transition from a-Si:H to fully μc-Si growth occurs at a hydrogen partial pressure of 0.5 Pa,[10] and roughly a factor of 2 lower for deuterium.[11]

For the photocapacitance and photocurrent studies described below, we evaporated semitransparent Pd contacts onto each film and reverse biased the junction at the p^+ c-Si substrate. Samples were studied in ''state *A*'' (annealed in the dark at 470 K for 30 min) and in a light soaked ''state *B*,'' produced by exposure to a tungsten-halogen light source at an intensity of 300 mW/cm^2 for 150 h.

We previously utilized Raman spectroscopy to establish the existence of a μc-Si component for each of these samples.[12] This method also allowed us to estimate the relative volume fractions of crystallites in these samples. More information about the detailed structure of these films was obtained using TEM. An example of the film structure is shown in the bright-field image presented in Fig. 1. A selected area diffraction pattern from the region indicated by the circle confirms that the dark regions are actually composed of small crystallites, which give rise to the ring pattern. Dark-field microscopy using a portion of a ring confirmed that small 5–50-nm-sized crystallites had agglomerated to form the dark regions shown in Fig. 1.

To probe the electronic properties of these samples, we recorded the sub-band-gap spectra obtained via the transient photocapacitance (TPC) and transient junction photocurrent (TPI) methods.[13,14] Because the TPC method detects the optically induced charge change within the depletion region while the TPI method detects the charge motion, these two

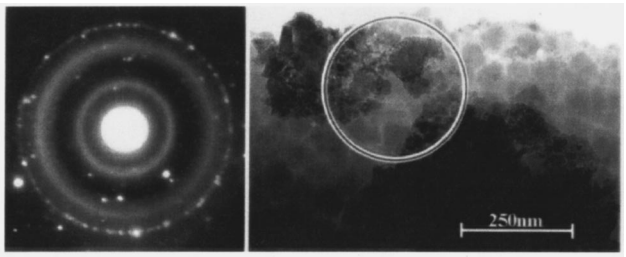

FIG. 1. Bright-field TEM image of sample 1. The diffraction pattern from the region circled indicates that the dark regions in the micrograph consist of fine-grained crystalline Si material.

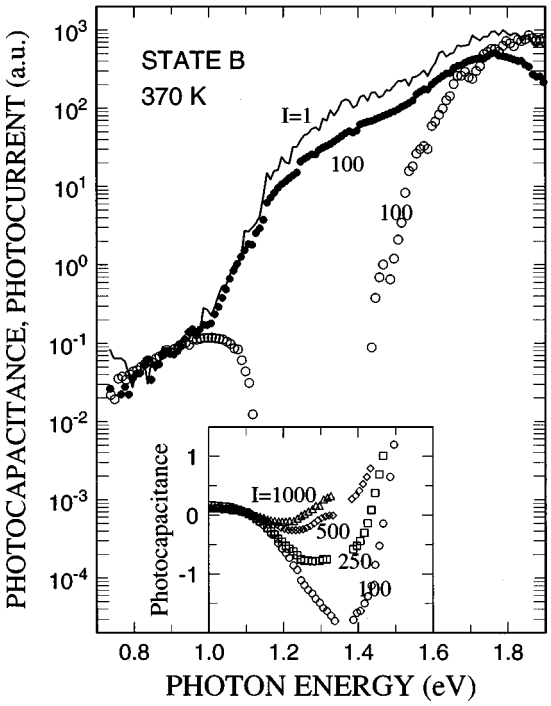

FIG. 2. Photocapacitance and photocurrent spectra of sample 1 in its light-soaked state. The photocurrent spectra (at two light intensities) are denoted by the solid line and filled circles, while the photocapacitance spectra are denoted by the open symbols (at four light intensities). The inset shows the intensity dependence of the photocapacitance in more detail on a *linear* scale. In all cases the back (c-Si) junction was biased at -2.3 V, and the filling pulse reduced this to -0.3 V. The absolute intensities vary with optical energy; however, $I=1$ corresponds to $1.7\times10^{12}\,\mathrm{cm}^{-2}\,\mathrm{s}^{-1}$ at 1.3 eV.

methods provide complementary information to sort out the types of transitions that occur. In particular, a transition between a gap state to the majority (conduction) band will *increase* the junction capacitance, while those to the minority band will *decrease* the capacitance. Thus, the TPC spectra reflect the difference *between* these two types of transitions. In contrast, the sign of the current arising from either type of transition is the same, so that the TPI spectra reflect the *sum*.

The spectra in either case are obtained by averaging the signal over a particular time window following a voltage filling pulse, and are taken alternately with and without the presence of the sub-band-gap light to determine the difference signal. This is then normalized to the photon flux. Examples of the TPC and TPI spectra of one sample in its light-soaked state at several intensities are shown in Fig. 2, in which the two types of spectra have been overlapped in the lowest energy regime (below 0.9 eV). As discussed in detail elsewhere,[14] this alignment relies on the fact that only majority carrier transitions will be possible at optical energies less than half the gap; thus the current and capacitance signals should be strictly proportional. We note that the TPI and TPC signals in this energy regime scale linearly with the light intensity so that these normalized spectra appear independent of intensity.

The spectral dependences below optical energies of 1.0 eV and above 1.6 eV are quite consistent with many such previous spectra reported for a-Si:H,[14] indicating transitions from the dominant deep defect band and the band-tail region,

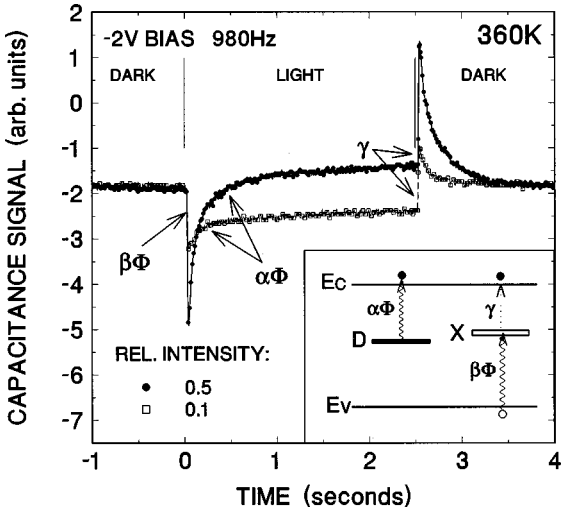

FIG. 3. Capacitance transient data for sample 1 at two different light intensities using 1.3 eV light. Note the two types of optical excitation processes that occur during the light-on region: a fast process (labeled $\beta\Phi$) that decreases the junction capacitance, and a slow process (labeled $\alpha\Phi$) that increases the capacitance. When the light is turned off, a fast thermal process (labeled γ) reverses the change caused by the fast optical process. The inset indicates our proposed model for the types of processes which account for the observed changes in capacitance. [Note: For the photocapacitance *spectral* measurements (e.g., Fig. 2) a voltage ''filling pulse'' of 10–100 ms duration is inserted at the beginning of each light and dark period to refill any majority carrier traps. Here this pulse has been omitted so that it will not obscure the appearance of the fast transients due to the X defects. Such a filling pulse greatly speeds up the slow recovery transient appearing in the dark.]

respectively. However, in the intermediate energy regime, 1.0–1.5 eV, these spectra reveal a feature that is never observed in standard glow discharge a-Si:H samples. Because this feature has a threshold close to the c-Si band gap and, moreover, is roughly proportional to the integrated crystalline Raman component for this series of samples,[12] we believe it is associated with the crystallites contained within these films. This feature exhibits two other interesting attributes. First, it results in a negative photocapacitance signal, implying a dominance of a minority band transition. Second, the dependence on light intensity due to this feature for both the TPC and TPC spectra is markedly *nonlinear*. This is reflected in Fig. 2 by the fact that the spectra for different light intensities no longer overlap as they do for the lower optical energies.

In Fig. 3 we display actual capacitance transients, alternatively with and without the presence of 1.3 eV light (the energy where this feature is most prominent). Here we clearly observe the presence of two distinct types of optical transitions, a fast component which *decreases* the capacitance as soon as the light is turned on, and a component that *increases* the capacitance much more slowly. Once the light is turned off, the faster component of the capacitance change is reversed within a few milliseconds. A schematic proposing the key transitions responsible for these transients is shown in the inset. It indicates that two distinct gap levels are involved, labeled D and X.

We record the photocapacitance over a time window that typically extends between 0.3 and 0.7 s following the onset

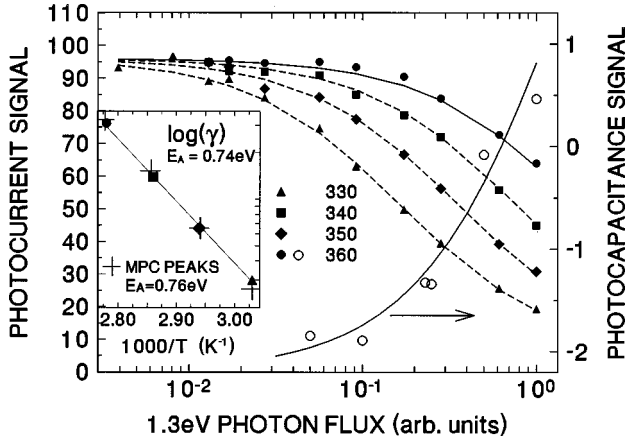

FIG. 4. The intensity dependence of the normalized photocapacitance and photocurrent spectra at 1.3 eV for state *B* of sample 1. The highest light flux was $4.5\times10^{15}\,\mathrm{cm^{-2}\,s^{-1}}$. The solid lines are fits to the 360 K data based upon the set of optical transitions shown in the inset of Fig. 3 The dashed lines are fits to the photocurrent spectra at several other temperatures obtained by only allowing the thermal rate parameter γ to vary. The inset indicates that γ is thermally activated (solid symbols), and that its temperature dependence closely matches that of the peak of the modulated photocurrent spectra of Fig. 5 (crosses).

of illumination. This means that steady-state conditions (between optical filling and thermal emptying) have been achieved for the fast component (X), while the optical emptying of the slow component (D) is still in its initial stage. Comparing the transients for the two light intensities displayed in Fig. 3 also indicates that the magnitude of the capacitance change for D is nearly linear with intensity, but markedly sublinear for X. This indicates that the optical excitation in the latter case is approaching saturation.

The normalized photocapacitance as well as the photocurrent signals obtained in this manner are displayed over a much wider range of light intensities in Fig. 4. The photocurrent signal dependence is also shown for several lower temperatures at which, unfortunately, the photocapacitance signals cannot be accurately measured because of the greatly increased ac response times. These intensity dependences can be fit quite well based upon the set of transitions indicated in the inset to Fig. 3, which are described in detail below.

Level D is occupied in thermal equilibrium and the subband-gap light excites electrons from D and into the conduction band at the rate $\alpha\Phi$, where Φ denotes the optical flux. Since this rate is slow relative to the time delay, τ, before the experimental window, this implies the *loss* of $\alpha\Phi\tau N_D$ electrons per unit volume from these states (relative to the sample in the dark). Level X is unoccupied in equilibrium and the light excites valence-band electrons into these states at a rate $\beta\Phi$. However, these electrons are lost by thermal excitation to the conduction at a rate γ. Since steady-state conditions have been reached by time τ, the electronic occupation fraction of level X will be given by $f=\beta\Phi/(\beta\Phi+\gamma)$. This corresponds to the *addition* of fN_X electrons per unit volume into the gap. Thus, the TPC signal will be proportional to the total charge change normalized to the flux, or

$$S_{\mathrm{TPC}}\propto\alpha\tau N_D-\frac{\beta}{\beta\Phi+\gamma}N_X. \tag{1}$$

The corresponding TPI signal due to these transitions states will be proportional to the density of electrons inserted into the conduction band per unit time plus a fraction, ξ, of the number of holes (limited by their lower mobility). Neglecting any significant hole insertion via the mostly filled D levels, one has, therefore,

$$S_{\mathrm{TPI}}\propto\alpha N_D+\frac{\beta\gamma}{\beta\Phi+\gamma}N_X(1+\xi). \tag{2}$$

Since the parameters τ and ξ can be determined independently, and we have normalized both signals to the same value at low optical energies (which sets the constants of proportionality), this leaves only four parameters to fit the TPC plus TPI signals versus photon flux (α, β, γ, and the ratio N_x/N_D).

The fits obtained are displayed along with the data in Fig. 4. The TPC and TPI fits at 360 K are determined from a common set of these parameters, and the TPI data at the lower temperatures have been obtained by changing only the value of γ, the thermal escape rate for the electrons from X. The variation of the γ values with T is shown in the inset, indicating an activation energy of 0.74 eV. However, we note that this value should be viewed as a lower limit in the case that the optical cross section β also varies significantly with temperature.

The success of this simple model to fit the intensity dependence of both the TPC and TPI spectra leaves little doubt as to its validity. However, the origin of the levels D and X has not yet been discussed. We believe that the D level arises from bulk defects in the a-Si:D host material including, perhaps, an excess of such defects in the vicinity of the microcrystallites. Indeed, the value of the fitting parameter α is quite consistent with the optical cross section determined for deep defects in a-Si:H [of $(1-3)\times10^{-16}\,\mathrm{cm^2}$ (Ref. 13)]. The optical cross section for X, on the other hand, appears to be much too high for a normal point defect. First of all, the raw capacitance transient data (e.g., Fig. 3) indicate a rate faster than $(10\ \mathrm{ms})^{-1}$ at a photon flux near $3\times10^{15}\,\mathrm{cm^{-2}\,s^{-1}}$. This implies an optical cross section of at least $10^{-14}\,\mathrm{cm^{-2}}$.

Second, we know that this transition can be saturated at relatively high temperatures while competing with a thermal process having an activation energy 0.74 eV. To check whether this thermal process might be unusually weak due to a low preexponential factor, we carried out modulated photocurrent (MPC) measurements[15] to establish directly the thermal emission characteristics of the predominant electron traps in this sample. These spectra are displayed in Fig. 5 and utilize the same set of measurement temperatures employed in the TPI versus light intensity measurements. The MPC spectral peak dependence on temperature is shown in the inset to Fig. 4 on top of the Arrhenius plot for γ. We see that it exhibits a nearly identical activation energy of 0.76 eV. (Note that this differs from the 0.65 eV MPC feature usually dominating a-Si:H samples.[16]) The prefactor for the MPC peak is $1\times10^{13}\,\mathrm{s^{-1}}$. Therefore, if we identify this peak in the

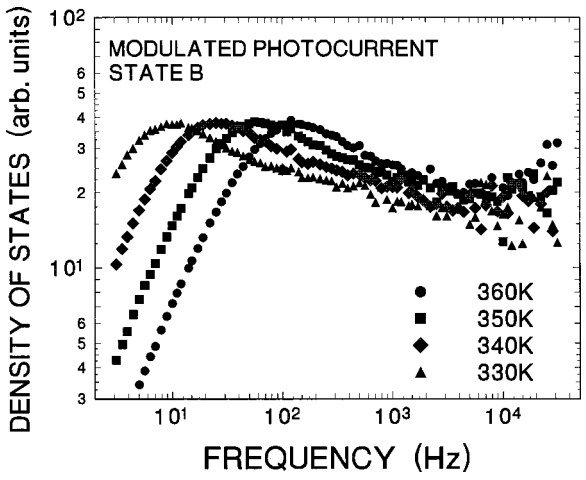

FIG. 5. Modulated photocurrent spectra for sample 1 in state *B*. The four temperatures used match those employed for the transient photocurrent measurements displayed in Fig. 4.

electron trap distribution with *X*, this establishes the absolute magnitude of γ and we obtain an optical cross section of $4 \times 10^{-14}\,\mathrm{cm}^{-2}$.

Given that the optical threshold for *X* lies very near the *c*-Si band-gap energy, it is appealing to hypothesize that *X* is populated via interband transitions in the embedded crystallites. The electrons introduced into the conduction band of the crystallites might then be trapped at defects near the crystallite/amorphous silicon host interface. Such a scenario might also help account for the unusually large effective optical cross section. It is also supported by the observation that β appears to increase by roughly a factor of 5 between the light soaked and annealed states of this sample, while the density, N_X, decreases by a similar factor. That is, the rate of optically generated electrons within the crystallites would remain nearly the same, but would be getting trapped onto fewer defects at the interface.

It is possible that the defect that we have discovered may have a significant impact on the performance of amorphous silicon devices fabricated from material near this mixed phase boundary. Such material is now known to lead to more stable solar cells;[6] however, once the crystalline fraction becomes appreciable, the device performance suffers.[8] Additional studies will hopefully help clarify the role this defect may have with respect to phototransport processes in amorphous silicon.

We wish to thank Hao Lee and Pete Sercel at the University of Oregon for carrying out Raman measurements on several of these samples. We also acknowledge useful discussions with Yoram Lubianiker. This work was supported by NSF Grant No. DMR-9624002 at Oregon and, at Illinois, by the Joint Services Electronics Project, through Dr. Al Goodman of the Office of Naval Research, and DOE Contract No. DEFG02-91-ER45349.

[1] F. Morin and M. Morel, Appl. Phys. Lett. **35**, 686 (1979).
[2] Z. Iqbal, A. P. Webb, and S. Veprek, Appl. Phys. Lett. **36**, 163 (1980).
[3] T. Hamasaki, H. Kurata, M. Hirose, and Y. Osaka, Appl. Phys. Lett. **37**, 1084 (1980).
[4] R. Richter and L. Ley, J. Phys. (Paris), Colloq. **42**, C4-261 (1981).
[5] R. Tsu, J. Gonzalez-Hernandez, S. S. Chao, S. C. Lee, and K. Tanaka, Appl. Phys. Lett. **40**, 534 (1982).
[6] D. V. Tsu, B. S. Chao, S. R. Ovshinsky, S. Guha, and J. Yang, Appl. Phys. Lett. **71**, 1317 (1997).
[7] J. H. Koh, Y. Lee, H. Fujiwara, C. R. Wronski, and R. W. Collins, Appl. Phys. Lett. **73**, 1526 (1998).
[8] S. Guha, J. Yang, D. L. Williamson, Y. Lubianiker, J. D. Cohen, and A. H. Mahan (unpublished).
[9] M. Pinarbasi, M. J. Kushner, and J. R. Abelson, J. Appl. Phys. **68**, 2255 (1990).
[10] G. Feng, M. Katiyar, Y. H. Yang, J. R. Abelson, and N. Maley, in *Amorphous Silicon Technology—1992*, edited by M. J. Thompson, Y. Hamakawa, P. G. LeComber, A. Madan, and E. A. Schiff, MRS Symposia Proceedings No. 258 (Materials Research Society, Pittsburgh, 1992), p. 179.
[11] J. E. Gerbi, P. Voyles, J. M. Gibson, and J. R. Abelson, in *Amorphous and Microcrystalline Silicon Technology—1998*, edited by R. Schropp, H. M. Branz, M. Hack, I. Shimizu, and S. Wagner, MRS Symposia Proceedings No. 507 (Materials Research Society, Pittsburgh, 1998), p. 429.
[12] D. Kwon, H. Lee, J. D. Cohen, H.-C. Jin, and J. R. Abelson, J. Non-Cryst. Solids **227-230**, 1040 (1998).
[13] A. V. Gelatos, J. D. Cohen, and J. P. Harbison, J. Non-Cryst. Solids **77&78**, 291 (1985).
[14] A. V. Gelatos, K. K. Mahavadi, J. D. Cohen, and J. P. Harbison, Appl. Phys. Lett. **53**, 403 (1988).
[15] H. Oheda, J. Appl. Phys. **52**, 6693 (1981).
[16] G. Schumm and G. H. Bauer, Phys. Rev. B **39**, 5311 (1989).